

# SOLAR ACTIVITY: FLARES; CMEs; SEPs; SOLAR WIND

N. Vilmer<sup>1</sup>

<sup>1</sup>DASOP-URA CNRS 8645, Section d'Astrophysique de Meudon,  
Observatoire de Paris, 5 Place J. Janssen, 92195- Meudon Cedex, France

## ABSTRACT

In this paper, the different aspects of solar activity which influence the state of the terrestrial space environment are briefly reviewed. The main characteristics of these phenomena are briefly described, some examples of their observations are presented and a brief description of the physical processes that they involve is done. The paper refers to other publications in these proceedings for the specific aspects of predicting solar activity and related geomagnetic effects.

Key words: sun; solar activity and flares; solar wind; space weather.

## 1. INTRODUCTION

This paper briefly reviews the different phenomena related to solar activity which can affect our space environment: i.e. which determine the amount of solar flux impinging on the Earth, the level of geomagnetic activity and/or the production of energetic particles reaching the earth's orbit. The X/UV flux is dependent on the phase of the solar cycle and on the number of active regions. More dramatic variations of this ionizing flux are connected with the occurrence of solar flares. Flares also result in the production of energetic particles (electrons and ions) which either interact in the solar atmosphere where they produce a wealth of electromagnetic radiation or escape in the interplanetary space where they can propagate, be reaccelerated in the interplanetary medium and finally reach the terrestrial orbit. The solar wind which is the flow of ionized plasma continuously escaping from the solar corona and pervading the whole interplanetary space also induces geomagnetic activity by variations of its pressure and magnetic field. Magnetic field structures filled with ionized coronal plasma (Coronal Mass Ejections or CME's) are often ejected in the interplanetary medium with velocities reaching a few hundred kilometers per second (or even more). CME's can be observed in connection with flares but are also produced in the absence of flares in the case of coronal magnetic field configuration. They are also associated with the acceleration of energetic protons which can potentially reach the

terrestrial orbit. The occurrence of solar flares, of coronal mass ejections and of associated shock waves create perturbations in the interplanetary medium. The production of solar wind streams with different velocities is at the origin of corotating interaction regions and shocks. All these perturbations in the interplanetary medium must be considered when analyzing the propagation of energetic particles. In this paper, the main characteristics of the above phenomena are briefly overviewed and some relevant observations are presented. The forecasting of these phenomena as well as space weather predictions are extensively discussed in these proceedings and shall only be briefly mentioned here.

## 2. SOLAR ACTIVITY AND VARIABILITY

### 2.1. Solar Activity and Variability at Photospheric and Chromospheric Levels

The oldest evidence of solar variability and activity was obtained from the observations of the varying sunspot numbers on the solar surface dating back to the 17<sup>th</sup> century. Figure 1 shows the average daily sunspot area from 1870 to these days. The number of sunspots follows an irregular cycle of about 11 years with some obvious long-term changes that will not be discussed here. The solar cycle is linked to the solar dynamo, i.e. the generation of the solar magnetic field and the oscillation of its large scale configuration between a dipolar component at the solar minimum and a configuration with a strong quadrupolar configuration giving rise to sunspots at the solar maximum. When looking at the large scale magnetic field direction, the mean duration of the cycle is in fact 22 years since every 11 years a reversal of the dipolar magnetic field is observed. Different methods of predicting sunspot cycles are presently used (see e.g. Lantos, Michard in these proceedings).

Other means of observing the solar cycle and the level of activity is to follow the evolution with time of the solar atmosphere at different heights. Figure 2 shows observations of the solar atmosphere performed at three optical wavelengths which are formed in media with different densities and temperatures, i.e. at different heights of the solar atmosphere. H $\alpha$  emission comes indeed from chromospheric levels, i.e. from a relatively cold ( $T \simeq 6 \cdot 10^3$  K) but dense ( $n \simeq 10^{11}$

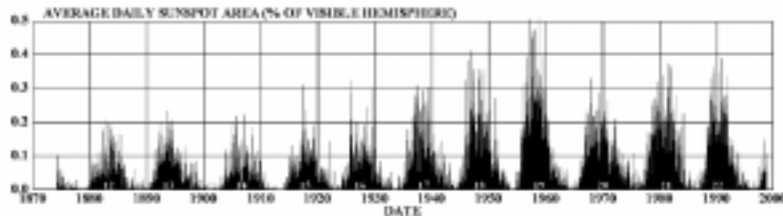


Figure 1. Average daily sunspot area measured since 1874 up to nowadays at the Royal Greenwich Observatory (adapted from <http://science.nasa.gov/ssl/pad/solar/images/bfly.gif>)

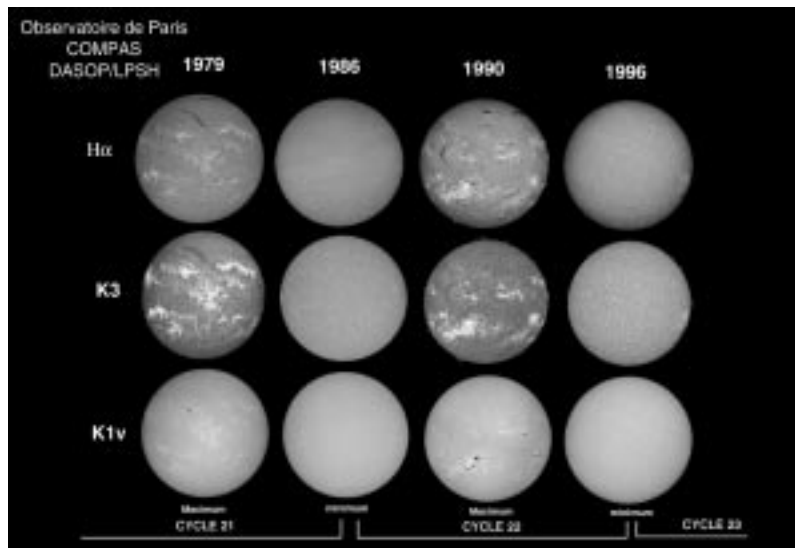


Figure 2. Observations of the solar atmosphere at 3 optical wavelengths showing the evolution of the activity with the cycle (observations performed by COMPAS at the PARIS Observatory/DASOP/LPSH- Courtesy of COMPAS).

-  $10^{12} \text{ cm}^{-3}$ ) layer of the solar atmosphere located around 1000 km above the solar surface. The emission produced in the blue wing of the K line of CaII (K1v) comes from an even colder layer deeper in the atmosphere while the emission produced in the center of this line (K3) arises from layers slightly above the  $H\alpha$  formation one. Observations at different wavelengths thus allow to probe the solar atmosphere at different heights. Figure 2 shows such observations for two successive solar cycles around the time of maximum and minimum activity. While the emission in K1v allows to observe dark sunspots as well as bright chromospheric plages at the time of maximum activity (1979 and 1990), the observations performed in  $H\alpha$  or in K3 reveal the bright emission of the active regions as well as the dark chromospheric features (especially seen in  $H\alpha$ ) (filaments) corresponding to chromospheric material magnetically embedded in the hotter and higher altitude corona.

## 2.2. Solar Activity and Variability at Coronal Levels

The corona which is a hot ( $T \approx 10^6 \text{ K}$ ) and tenuous plasma ( $n \approx 10^8 - 10^{10} \text{ cm}^{-3}$ ) produces X-ray and radio emission. Figure 3 shows full-disk obser-

vations of the solar corona performed at radio and X-ray wavelengths at a period close to the solar minimum (October 1996) (left) and in the rising phase of the present cycle (March 1997) (right). The bright active regions seen at optical wavelengths (see e.g. Figure 2) are also seen in X-rays and even at radio wavelengths (Figure 3 left). However, additional magnetic features are seen at coronal levels (i.e. dark features in X-rays and radio in Figure 3 left). They correspond to coronal holes which are seen e.g. for the image close to solar minimum, at the north pole as well as extending towards the solar equator (see the X-ray and radio images in Figure 3 left). While active regions are related to the small scale magnetic fields at the surface of the sun, coronal holes are the signature of the solar magnetic field structures at larger scales which will ultimately structure the interplanetary medium. Coronal holes correspond to colder and less dense regions in the corona (see David et al 1997 for recent measurements of the temperature of coronal holes) and underlines the region of the corona where magnetic field lines are open to the interplanetary space. They are believed to be the source of the fast solar wind (see section 6). Equatorial coronal holes such as the ones shown in Figure 3 are relatively frequent at the time of the minimum of solar activity. The regime of fast solar wind that they produce is responsible for recurrent( with

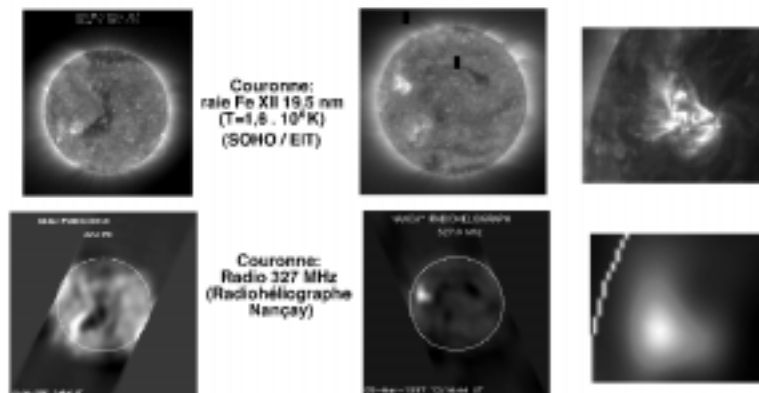


Figure 3. Observations of the solar corona in X/UV by SOHO/EIT (Courtesy of SOHO/EIT) (FeXII line at 19.5nm) (top) and at radio wavelengths (327 MHz) by the Nançay Radioheliograph (NRH) (bottom). The images on the left correspond to a period close to the solar minimum (October 1996). On the right the images and a zoom on the active region close to the east limb were performed in the rising phase of the present cycle (March 1997). (SOHO is a project of international cooperation between ESA and NASA.)

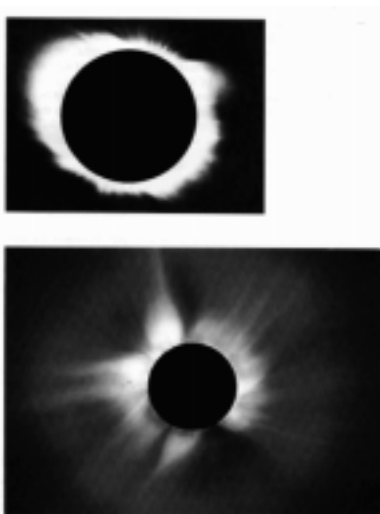


Figure 4. Minimum (top) and maximum (bottom) corona observed during total eclipses (from Stix 1989 , photographs taken by E.E. Barnard and G.W. Ritchey (top), G.A. Newkirk (bottom, Courtesy NCAR, Boulder)

a period of 27 days linked to the solar rotation) geomagnetic activity observed primarily at the time of minimum activity. In such a case of an equatorial coronal hole stable for many rotations, it is possible to perform some prediction of geomagnetic activity. Before the advent of radio and X-ray observations the corona could be observed during total eclipses or with the help of coronagraphs which creates artificial eclipses. The white light emission which is then observed is not the radiation emitted by the corona itself but represents the Thomson scattered emission of the photospheric light and thus reflects the density in the coronal structures. The shape of the corona is also closely related to the shape of the solar magnetic field and is strongly dependent on the phase of the cycle. At the solar minimum, the corona is elongated along the solar equatorial direction and also reveals

the existence of " solar plumes " which are thin hair like structures seen at the pole. At the maximum, the corona appears as much more structured and shows the existence of streamers which can be observed up to several solar radii( Figure 4). The coronal streamers are 5 to 10 times denser than the rest of the corona and are the tracers of the inversion line of the coronal magnetic field. At low coronal height, the base of the streamers probably consist of clusters of low altitude dense coronal loops surrounded by open magnetic field lines which are one of the possible sites of the slow solar wind. At higher altitudes, the open magnetic field lines anchored in different polarities of the global solar magnetic field delineate a plasma and a current sheet in the heliosphere. Observations of the corona performed at radio wavelengths allow to trace the signature on the disk of the plasma sheet

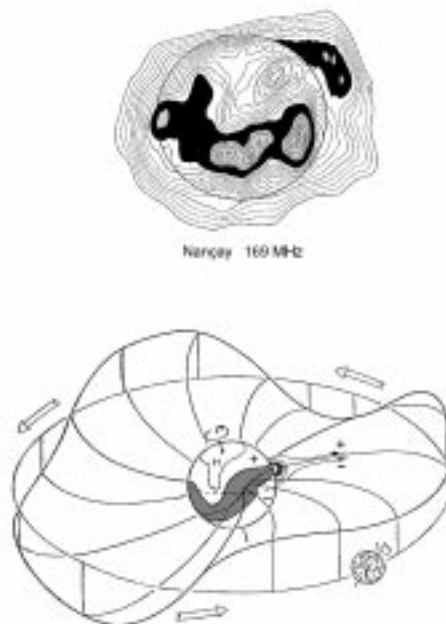


Figure 5. Top: Contour map of the quiet sun obtained via synthesis aperture at 164 MHz with the NRH in July 1984 (from Lantos, P. Alissandrakis, C.E. 1999). The dark contours show the coronal plateau corresponding to the signature of the plasma sheet on the disk. It is brighter than the average quiet corona. The grey contours on the coronal plateau show localized brighter sources. The dark region on the north-west limb also corresponds to the plasma sheet. The oscillation of the streamer belt from one hemisphere to the other is clearly evidenced by the location of the dark regions on the map. Bottom: large scale organization of the magnetic field in the heliosphere and relationship with the coronal structures and the coronal plateau (adapted from Schwenn 1986; Courtesy of Lantos, P.)

associated with the coronal streamer belt (Figure 5). The denser region of the corona associated with the low altitude loops at the base of the coronal streamer produces indeed an increased emission (see the dark feature on figure 5 close to the solar equator). The oscillation of the streamer belt from one solar hemisphere to the other is clearly seen on this figure. The shape of the streamer belt will ultimately structure the interplanetary magnetic field and the interplanetary sectors as seen from the Earth (i.e. regions in which the interplanetary magnetic field has a north and south polarity (Figure 5b).

### 2.3. Solar Irradiance Variations

Even if the appearance of the sun is highly variable from maximum to minimum activity, the variation of the total solar irradiance (i.e. the total flux integrated on the whole spectrum) averaged on a period of 30 days is only of the order of 0.1 % from maximum to minimum activity (see e.g. Willson 1999). The variation is however much more pronounced in the X/UV domain for which the radiation is not only produced by the quiet solar atmosphere but also in the coronal loops above active regions and is thus very dependent on the level of solar activity. The amount of UV flux ionizing the earth's atmosphere is thus strongly related to the number of solar sunspots. As shall be seen in the next section, the variation of the X/UV flux is still much larger in the case of solar flares where it can be magnified by several orders of

magnitude. The X/UV flux is one of the three factors in the Solar-Terrestrial Connection. The absorption of the highly variable X/UV flux by the Earth's atmosphere modifies not only the ionization of the atmosphere and the equilibrium of the different ionized components but also the neutral density in the high terrestrial atmosphere.

### 3. Solar Flares

Flares have been originally (since a century and a half) observed at optical wavelengths and many of them have been detected in the  $H\alpha$  line emission. In these optical lines, the occurrence of a solar flare leads to a sudden and localized increase of the emitted radiation. Flares usually occur in active regions, in the vicinity of sunspots, even if a significant fraction (about 10%) occur elsewhere. They are generally believed to result from the sudden release of magnetic energy in the corona on timescales ranging from a few minutes to a few hours. Most of the effects of flares are seen at coronal or chromospheric levels and correspond to an increase of the X-ray and radio emission in the solar corona as well as to  $H\alpha$  brightenings. Only a fraction of flares is seen in "white-light", i.e. as a localized increase of the solar photospheric emission in the continuum.  $H\alpha$  flares are systematically observed by an international network of observatories. Although the area of the  $H\alpha$  brightening is localized and reaches in the largest flares only 1/400

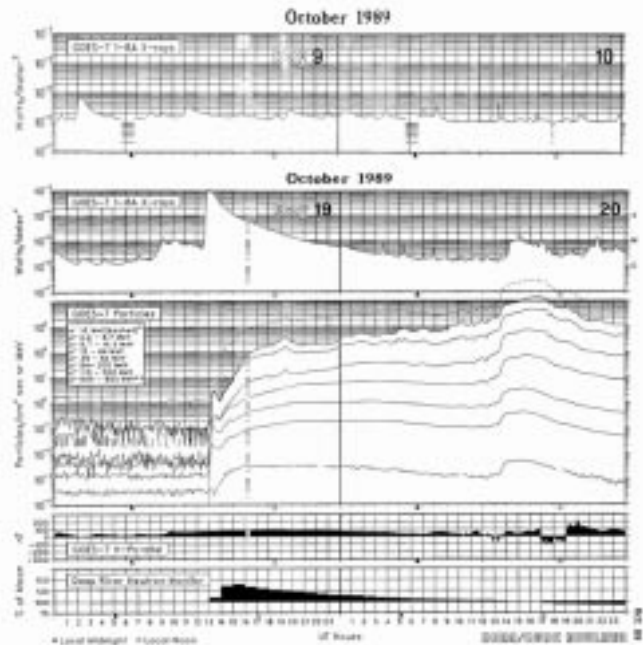


Figure 6. Top: Time profile of the soft X-ray flux in the 0.1-0.8 nm range recorded by GOES for two days in a relatively quiet period. Bottom: Time profile of the X-ray flux showing a large X-ray flare on October 19 1989; Measurements by GOES of the particle flux impinging on the earth and of the perturbations of the terrestrial magnetic field. Observations of a GLE event by the ground-level neutron monitors in close coincidence with the X-ray flare (adapted from *Solar Geophysical Data*, NOAA prompt reports).

of the solar surface, the effects of a flare can affect the corona up to a quarter of the Sun or even more (in particular in connection with coronal mass ejections, see Section 4).

At soft X-ray wavelengths (in the 0.1-0.8 nm band), flares are nowadays also continuously monitored by a series of geostationary american spacecrafts (GOES). As seen in figure 6, the variation of the soft X-ray flux is of one order of magnitude for the most common flares (C-class flares) but can reach two or even three orders of magnitude for the most energetic but less frequent M and X flares ( $\approx 100$  M flares a year and  $\approx 10$  X flares a year at solar maximum). Flares are of course related to the solar cycle and Figure 7 shows the variability of the flare rate seen at different wavelengths as a function of the level of the activity cycle (Aschwanden, 1999). The energy which is released during flares varies from  $10^{28}$  to  $10^{34}$  ergs. The released magnetic energy is transformed into : 1) thermal energy (localized heating leading to an increased brightness of e.g. the  $H\alpha$  and X-ray emission), 2) particle kinetic energy leading to the acceleration of electrons to energies of 10's keV to 1 GeV and ions to energies from a few MeV/nuc to GeV/nuc, 3) mechanical energy leading to several kinds of plasma ejecta, filament or prominence eruptions or even coronal mass ejections. It has been shown (see e.g. Wu et al, 1985) that a significant fraction of the released energy is manifested in the form of energetic particles which produces when interacting with the solar atmosphere a wide spectrum of emission ranging from metric/decimetric radio emissions, microwaves, hard X-rays and finally gamma-rays. Direct charged

particle and neutron observations in space and with ground-based monitors can also be associated with the occurrence of large solar flares (see figure 6). Perturbations of the terrestrial magnetic field are also observed in close connection with big flares. There is however a long-standing discussion on whether the most important feature of solar activity directly connected to large geo-effective proton events is really the solar flare phenomenon or rather linked to coronal mass ejections (see Section 4).

#### 4. Coronal Mass Ejections

Coronal Mass Ejections (CME's) have been first identified in the 1970s in observations with space-borne coronagraphs. They correspond to massive expulsions of plasma from the solar atmosphere and are the cause of major transient interplanetary disturbances that in turn have significant terrestrial effects. Several thousands of coronal mass ejections have now been observed in white light by space borne (Skylab, Solwind, Solar Maximum Mission and nowadays SOHO/LASCO) and ground-based coronagraphs. They are seen as bright features that move outwards through the solar corona at speeds from 10 to about  $2000 \text{ km s}^{-1}$  (Hundhausen, 1999) and involve the expulsion of substantial quantities of plasma from large regions of the corona (Figure 8). CME's have a frequency of occurrence that varies by more than an order magnitude over the course of the 11-year solar activity cycle: while near solar activity

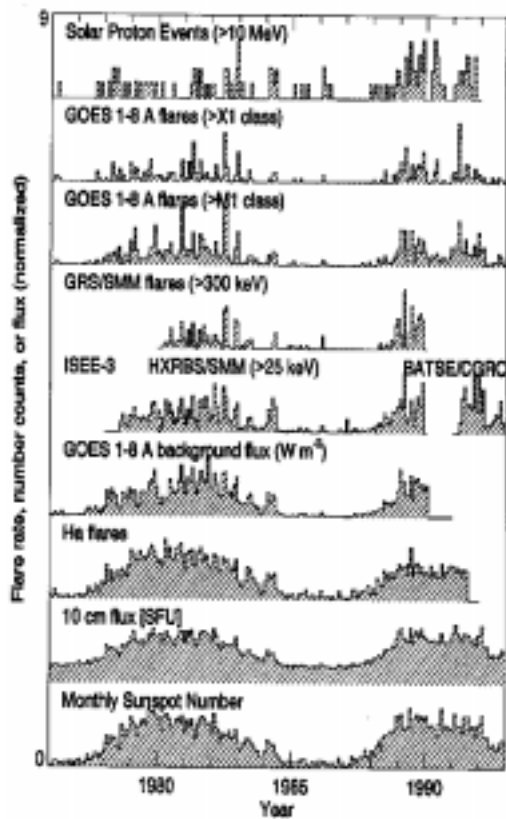


Figure 7. Compared variability of flare rates at X-ray, optical and radio wavelengths and of solar proton events (from Aschwanden, 1999).

minimum they occur at a rate of  $\approx 0.2$  events/day (Gosling, 1997), near solar activity maximum they occur at a rate of  $\approx 3.5$  events/day. Ejection masses are typically in the range from  $10^{15}$  to  $10^{16}$ g and the mechanical energy related to CME's ranges from  $10^{31}$  to  $10^{32}$  ergs.

Coronal mass ejections consist of three components: a bright frontal structure followed by a dark cavity and the dense prominence extended core. They are often associated with prominence eruptions, but many mass ejections are also observed without a prominence eruption or the disappearance of a dark filament from the visible disk. Equivalently, many coronal mass ejections are solar flare associated. However, such flare associations are less frequent than associations with prominence eruptions or other evidence for ejection of chromospheric material (Hundhausen, 1999). The relative timing of mass ejections and flares or prominence eruptions also may raise doubt that prominence eruptions or flares are the causes or "drivers" of coronal mass ejections. Rather these forms of activity may occur along with or after mass ejections onsets as a consequence of the magnetic changes that are also responsible of mass ejections (Hundhausen, 1999). On the other hand, a general question which can be raised concerns the transition between a relatively localized instability characterized either by a flare or by a filament disappearance to the large scale phe-

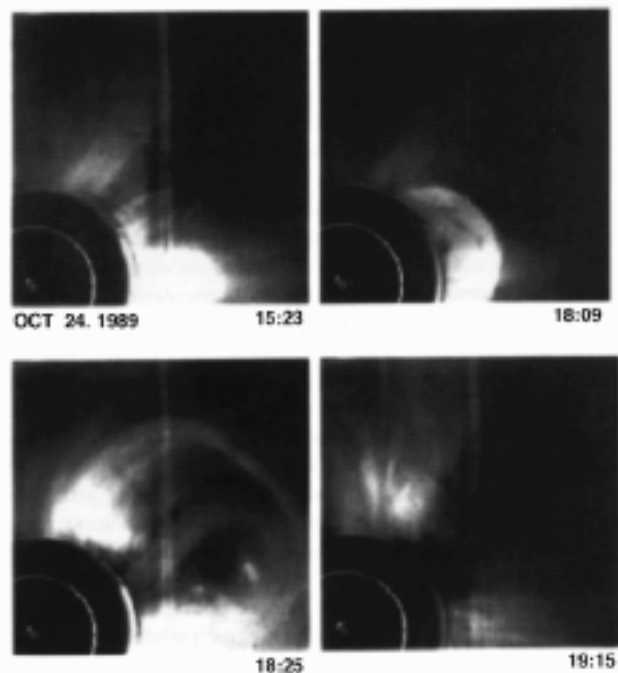


Figure 8. Time sequence of coronagraph images from SMM showing a coronal mass ejection (from Hundhausen 1999).

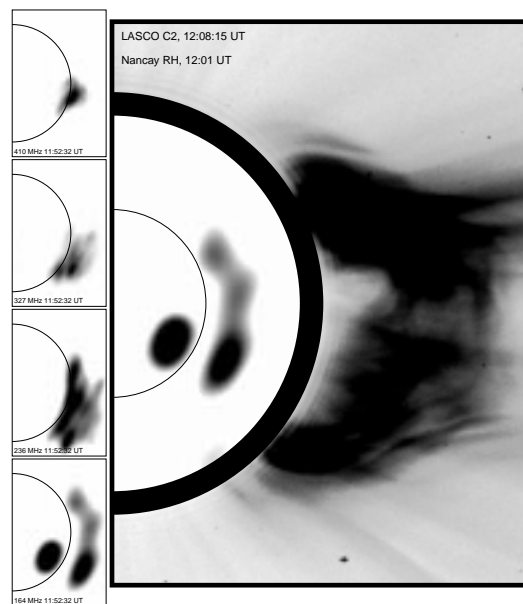


Figure 9. Left: Radio images recorded at 4 frequencies showing the development of the radio emitting sources observed with the NRH. Right: Composite image of the CME observed by LASCO/C2 and of the radio image at 164 MHz showing the good agreement between the spatial extent of the CME and of the radio sources (adapted from Maia et al, 1999)

nomenon of the coronal mass ejection seen in white

light coronagraphs. Recent combined observations of CME's and of signature of radio emission at the onset of CME's give some clues to this problem (Figure 9). The development of the fast CME observed by LASCO on November 6 1997 (speed of the leading edge of  $1700 \text{ kms}^{-1}$ ) implies in fact the brightening of an initial small scale hot loop seen in the FeXIV line with the inner LASCO coronagraph (Maia et al. 1999). This small, scale loop has a fast expansion and reaches after a few minutes a large angular extension. Such a fast development and extension from a relatively localized extension towards a large scale phenomenon is clearly seen when observing the radio emission (Figure 9). From 11:54:30 UT to 12:01:00 UT, there is indeed a spread of the radio sources initially localized in a small region in the vicinity of the flare site in the south hemisphere towards the northern one. The radio sources show the presence of accelerated electrons in the corona together with the development of magnetic instabilities associated with the CME. It can be also noticed that the final spatial extent drawn by the radio sources is consistent with the spatial extent of the CME seen by the second coronagraph (C2) of LASCO. This CME was at the origin of the arrival of energetic protons at the earth's orbit. It must be noticed that most of the CME's which propagate towards the Earth may not be so easily detected by coronagraphs which mostly see CME's close to the solar limb, i.e. at an angle of  $90^\circ$  from the Sun-Earth's direction. In these conditions, it is quite important to be able to detect CME's on the solar disk. Such a search has been recently performed with the Extreme Ultraviolet Imaging observations of EIT on SOHO (see e.g. Thompson et al., 1998). The comparison of images taken at  $\simeq 10$  minutes interval show in fact in many events the propagation on the solar disk of a coronal transient wave (see e.g. Figure 10 from Thompson et al 1998)) after an initial brightening of the coronal material close to an active region and in close temporal association with a soft X-ray flare. The wave then propagates across the solar disk with a speed of  $\simeq 250 \text{ kms}^{-1}$ . Such transient waves have been observed for many events and are often associated with white-light signatures in LASCO such as halo coronal mass ejections (see e.g. Plunkett et al 1998). Such observations can be used to detect the first signature of CME's onset on the disk for CME's propagating towards the earth. Coronal mass ejections are also associated with interplanetary shocks which generate type II radio emission at the local plasma frequency or its harmonic. As shown by Reiner et al. (1998) using WIND observations, these type II radio emissions provide a means of remotely studying and tracking CME's from the solar corona to the earth's orbit. In particular, looking at the radio emission in the 15 MHz-30 kHz frequency range allows to track the frequency drift of the interplanetary type II bursts, i.e. the propagation in the interplanetary medium of the shock associated with the leading edge of the CME. This could be used to predict the arrival time of the CME associated shock at the earth's orbit. As will be discussed in section 6, CME's are associated with peculiar signatures of disturbances in the interplanetary medium called ICME (Interplanetary Coronal Mass ejections). Finally, as in the case of solar flares, the coronal mass ejections are also associated with large energetic particle events in the interplanetary medium (see next section).

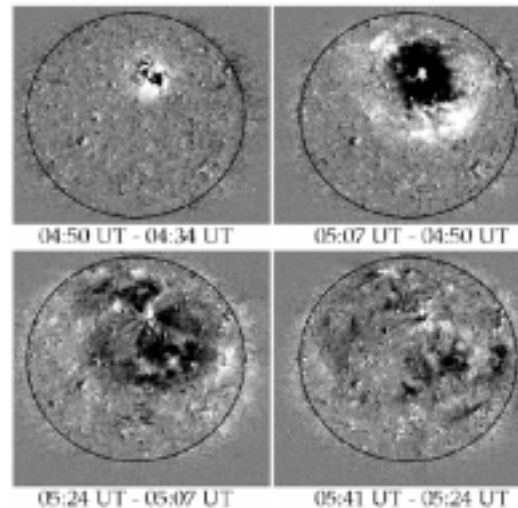


Figure 10. SOHO/EIT running difference images at 19.5 nm. showing the large scale wave transient associated with an earth-directed CME (from Thompson et al 1998)

## 5. Solar Energetic Particles

The transient production of relativistic particles associated with solar flares became evident with the discovery in 1942 of dramatic increases in the count-rates of several ground level cosmic-ray monitors (GLE or Ground Level Events)(see e.g. Figure 6 for an example of a solar energetic particle). However, since the discovery of coronal mass ejections, it became clear that the strong shocks driven by the fastest CME's are also quite effective in accelerating a small fraction of the coronal and solar wind particles to very high energies. For nearly 30 years, it was believed that all solar energetic particle (SEP's) were accelerated in solar flares and could afterwards diffuse across magnetic field lines to distant longitudes by coronal diffusion before impinging on the earth's orbit (see e.g. figure 7). However, it is now strongly believed that most major proton energetic events result from particle acceleration occurring in the outer corona and in interplanetary space at shocks driven by fast CME's (see e.g. Reames, 1996). New observations have indeed revealed that there are two distinct populations of solar energetic particles (called "impulsive or "gradual ") based upon the electron/proton ratio, abundances, ionization states, duration as well as longitude distribution of the events. In particular, the largest and most energetic particle events at earth are associated with small values of the e/p ratio and have on the average the same element abundances and ionization states as those in the ambient corona. Their duration is rather long (a few days), they are strongly associated with CME's (96 %) (Reames, 1996) and with interplanetary shocks. Their longitude distribution is rather broad ( $180^\circ$ ). Their occurrence is of the order of 10/year. These large proton events are the ones which correspond to most dramatic effects at the earth's level. They are generally associated with the observation of a specific type of coronal radio emission at metric and decametric wavelengths (type II and type IV bursts) which can be used as predictors of large SEP's. On the

other hand, the other class of SEP events is characterized by an increased electron to proton ratio and by increased ratio of e.g.  $^3\text{He}/^4\text{He}$  and  $\text{Fe}/\text{O}$  abundances. Moreover the ionization state is much larger than in the ambient corona suggesting that the particles come from a coronal heated plasma, such as the one encountered in flares. The duration of such events is only of a few hours at the earth's orbit and the distribution of longitude is relatively narrow (less than  $30^\circ$ ) and centered around the solar longitudes ( $\simeq 60^\circ$ ) for which there is a good magnetic connection with the earth. Such events are believed to be associated with flares, are more numerous ( $\simeq 1000/\text{year}$ ) but are probably less important in terms of space weather.

## 6. The Solar Wind and its Solar Activity Driven Perturbations

The corona is not gravitationally bounded to the sun and a flux of ionized matter, the solar wind, escapes continuously from the sun (see e.g. Hundhausen, 1995). It was first observed directly and definitively by space probes in the mid-1960s. The solar wind is significantly influenced by solar activity. It consists largely of ionized hydrogen. It also contains a weak magnetic field oriented in a direction nearly parallel to the ecliptic plane but at an angle of approximately  $45^\circ$  to the sun-earth direction at the earth's orbit. The solar wind carries mass away from the Sun at a rate of  $1.6 \cdot 10^{12} \text{ gs}^{-1}$  and energy at a rate of  $1.8 \cdot 10^{27} \text{ ergs}^{-1}$ . The solar wind is thus negligible in the overall mass and energy balance of the sun. The typical speed of the solar wind flow is  $400 \text{ kms}^{-1}$  at the earth's orbit. However, it was known since the first measurements and nowadays well demonstrated by the ULYSSES observations that two regimes of solar wind exist. The velocity of the solar wind ranges indeed from  $\simeq 300 \text{ kms}^{-1}$  (slow wind) up to  $700 \text{ kms}^{-1}$  (fast wind). These two regimes correspond also to different values of the solar wind plasma density. The high speed solar wind streams have their sources in the part of the solar corona where the magnetic field lines are open to the interplanetary space, i.e. in the coronal holes. There is a tendency for the high speed streams to recur after 27 days, which is the equatorial period of the rotation of the large scale solar magnetic field. The occurrence of these high speed streams has been found to be the source of recurrent geomagnetic perturbations. The succession of slow and fast solar wind regimes (according to the nature of the coronal structure from which the solar wind emanates) creates a stream interface in the interplanetary medium when the fast wind encounters the slower wind. This stream interface corresponds to a plasma compression and may also lead to the formation of shock waves upstream and downstream of the interface. These interplanetary shocks delimitate a corotating interaction region (CIR), sometimes already formed at the earth's orbit.

In addition to the recurrent solar wind variations that rotate with the Sun (see above) there are sporadic disturbances of the solar wind such as interplanetary shocks due to e.g. solar flares or CME's and magnetic clouds (also called ICME's). Such magnetic clouds correspond to a particular type of interplanetary dis-

turbances with the following properties: 1) the magnetic field direction rotates smoothly through a large angle during an interval of the order of one day; 2) the magnetic field strength is higher than average and 3) the temperature is lower than average (see Burlaga, 1991). Statistical evidence for an association between magnetic clouds and coronal mass ejections has been reported but the mapping from the coronal mass ejections observed close to the sun to the clouds in the heliosphere is far from being understood. It is indeed not known which coronal mass ejection will be seen in the solar wind as a magnetic cloud. Finally, as discussed in e.g. Chen et al (1997), there is a correlation between geomagnetic activity and the occurrence of a southward component of the interplanetary magnetic field. During the passage of an interplanetary magnetic cloud, the magnetic field is usually partly southward and an increase of geomagnetic activity is usually observed. It was for example found that 59% of the largest magnetic storms for which interplanetary data were available for 10 years from 1972 to 1982 were associated with magnetic clouds (see e.g. Burlaga, 1991). It is thus quite promising to develop methods for identifying and predicting the occurrence, onset, duration and geoeffectiveness of solar wind events using measurements upstream of the earth. However, to be able to predict more than one hour in advance would require to be able to detect and identify disturbances such as coronal mass ejections at the sun or as soon as they leave the sun and to find good criteria to forecast if these disturbances will ultimately lead to e.g. a geoeffective magnetic cloud.

## 7. General Conclusion

The different aspects of solar activity linked to the evolution at different temporal and spatial scales of the sun's magnetic structure have been reviewed in this paper. The disturbances of the interplanetary medium induced by flares or coronal mass ejections have been briefly described as well as some of their effects on the terrestrial environment. Concerning the prediction of the space weather and of the effects of the solar activity on the earth's environment, it is clear that, if today, different techniques and algorithms have been developed to predict in almost real time geomagnetic storms using e.g. solar wind measurements at the Lagrange point, the prediction of the state of the solar wind given the level of solar activity is much more empirical and still needs in most cases further development. In particular, if recurrent solar wind disturbances can be forecasted in advance, the prediction of more sporadic disturbances due to interplanetary shock waves or to CME's is more difficult. In particular, if the arrival time at the Earth of the disturbance can be predicted once a large solar flare or a CME is observed, the amplitude of the geomagnetic effect is largely unpredictable without the further development of an applied research field specifically dedicated to the space weather activity.

## Acknowledgements

The author is very grateful to Isabelle Buale and Monique Savinelli for their help in preparing the fig-

ures and wish to acknowledge useful discussions with P. Lantos and K.L. Klein

## REFERENCES

- Aschwanden M.J. 1999, in *The Many Faces of the Sun: A Summary of the Results from NASA's Solar Maximum Mission*, eds Strong, K.T., Saba, J.L., Haisch, B., Schmelz J.T. , 273
- Burlaga,L.F.E, 1991, in *Physics of the Inner Heliosphere: Particles, Waves and Turbulence*, eds Schwenn,R., Marsch,E. ,1
- Chen,J., Cargill, P.J., Palmadesso, P.J. 1997, *JGR* 102, A7-14701
- David,C., Gabriel,A.H., Bely-Dubau, F. 1997, *ESA, SP 404*, 319
- Hundhausen,A.J., 1995, in *Introduction to Space Physics*, eds Kivelson,M.G., Russell,C.T., 91
- Hundhausen,A. 1999,in *The Many Faces of the Sun: A Summary of the Results from NASA's Solar Maximum Mission*, eds Strong, K.T., Saba, J.L., Haisch, B., Schmelz J.T. , 143
- Gosling,J.T. 1997, in *Coronal Mass Ejections*, eds Crooker, N., Joselyn, J.A., Feynman, J., 9
- Lantos,P. 1997, *Le Soleil en face: le Soleil et les relations Soleil-Terre*
- Lantos,P., Alissandrakis, C.E., 1999, *A & A*, submitted
- Lantos,P., Michard,0 1999, these proceedings
- Maia,D., Vourlidis,A., Pick,M., Howard,R., Schwenn, R., Magalhaes,A. 1999, *JGR* in press
- Plunkett,S.P., Thompson,B.J., Howard,R.A., Michels,D.J., StCyr,O.C., Tappin,S.J., Schwenn,R., Lamy, P. 1998, *GRL* 25, 14-2477
- Reames,D.V. 1996, *AIP Conf Proc* 374, 35
- Reiner,M.J., Kaiser,M.L., Fainberg,G.J., Stone,R.G. 1998, *JGR* 103, A12-29651
- Schwenn,R. 1986, *Adv. Space Res.*, 1,3
- Stix,M. 1989, *The Sun: an Introduction*
- Thompson,B.J., Plunkett,S.P., Gurman, J.B., Newmark, J.S., St Cyr, O.C., Michels, D.J., Delaboudinière, J.P. 1998, *GRL* 25, 14-2461
- Willson, R.C. 1999, in *The Many Faces of the Sun: A Summary of the Results from NASA's Solar Maximum Mission*, eds Strong, K.T., Saba, J.L., Haisch, B., Schmelz J.T. , 19
- Wu, S.T., de Jager, C., Dennis, B.R., Hudson, H.S. and 17 co-authors 1986, *NASA Conference Publication*, 2439, 5-1